SCIENTIFIC REPORTS

OPEN

Thin single-wall BN-nanotubes formed inside carbon nanotubes

SUBJECT AREAS:
CARBON NANOTUBES AND FULLERENES
NANOWIRES
SELF-ASSEMBLY
MOLECULAR SELF-ASSEMBLY

Ryo Nakanishi[1], Ryo Kitaura[1], Jamie H. Warner[2], Yuta Yamamoto[3], Shigeo Arai[3], Yasumitsu Miyata[1] & Hisanori Shinohara[1]

[1]Department of Chemistry, Nagoya University, Nagoya, 464-8602, Japan, [2]Department of Materials, University of Oxford, 16 Parks Road, Oxford OX1 3PH, UK, [3]Ecotopia Science Institute, Nagoya University, Nagoya, 464-8603, Japan.

Received
14 December 2012

Accepted
18 February 2013

Published
5 March 2013

Correspondence and requests for materials should be addressed to R.K. (r.kitaura@nagoya-u.jp) or H.S. (noris@nagoya-u.jp)

We report a high yield synthesis of single-wall boron nitride nanotubes (SWBNNTs) inside single-wall carbon nanotubes (SWCNTs), a nano-templated reaction, using ammonia borane complexes (ABC) as a precursor. Transmission electron microscope (TEM), high angle annular dark field (HAADF)-scanning TEM (STEM), electron energy loss spectra (EELS) and high resolution EELS mapping using aberration-corrected TEM system clearly show the formation of thin SWBNNTs inside SWCNTs. We have found that the yield of the SWBNNT formation is high and that the most of ABC molecules decompose and fuse to form the thin BNNTs at a temperature of 1,673 K having a narrow diameter distribution of 0.7 ± 0.1 nm. Optical absorption measurements suggest that the band gap of the thin SWBNNTs is about 6.0 eV, which provide the ideal insulator nanotubes with very small diameters.

Nanotubes with a diameter of less than 1 nm provide the ideal nanospace to explore chemistry and physics in one-dimension. Single-wall carbon nanotubes (SWCNTs)[1–5], nano-scale cylinders consisting of single graphene sheet, are one of the most promising candidates for the fabrication of novel one-dimensional (1D) nanomaterials. To date, specific one-dimensional nanostructures, such as 1D crystalline array of molecules[6–12], metal complex nanowires[13–16] and metal atomic wires[17–19], have been created inside SWCNTs, in which the properties of these are substantially different from their bulk counterparts: spontaneous chiral symmetry breaking[20] and enlargement of magnetic moment[19]. However, the small band gap of SWCNTs typically ranging from 0 to about 1 eV[2,3] has so far precluded one from investigating the intrinsic optical and electronic properties of 1D nanostructures formed in SWCNTs. In addition, the small band gap of SWCNTs can lead to charge transfers between CNTs and 1D nanostructures, which modulate substantially their intrinsic structure and properties[21]. Therefore, the insulating nanotubes having a large band gap are definitely needed for detailed investigations of the intrinsic structure and properties of 1D nanosystems (supplementary Fig. S1).

Boron nitride nanotubes (BNNTs)[22–24] are intriguing nanotube materials consisting of hexagonal boron nitride sheets. One of the most important features of BNNTs is that BNNTs possess a large band gap (~6.0 eV) irrespective of the number of walls, diameters and chiralities[25–27]. In addition, BNNTs are chemically and mechanically stable[28]. Thin single-wall BNNTs (SWBNNTs) can, therefore, widely be used as an ideal nanotube for exploring nanoscience in 1D materials such as atomic wires[17–19,29]. Even though researchers have been trying to synthesize BNNTs by several methods including chemical vapor deposition[30–34], laser ablation[35–38], arc-discharge[39–42] and thermal decomposition of boron and metal nitrate[43], selective production of thin SWBNNTs has never been realized so far, which is in stark contrast to the presence of the well-established synthesis technique of thin SWCNTs[4,5].

Here, we report a novel synthesis method of thin SWBNNTs having an almost uniform diameter distribution of 0.7 ± 0.1 nm. Our strategy to synthesize thin BNNTs is to incorporate the so-called nano-templated reaction[14,18] using SWCNTs which we have developed during the past decade. The present high yield preparation of BNNTs using the nano-templated reaction is schematically shown in Figure 1. In this reaction, precursor molecules containing boron and nitrogen are encapsulated first in SWCNTs followed by a thermal decomposition/fusion reaction inside the SWCNTs. The key idea here is to use a 1D array of ammonia borane complexes (ABC) molecules as a reactant, and a confined space of SWCNTs as a template for expecting the SWCNTs accelerate the formation of SWBNNTs due to their structural affinity which is confirmed in the pioneering work on multi-wall boron nitride and carbon hybrid nanotubes[44,45]. These ideas lead to selective formation of thin BNNTs that have been difficult to synthesize in normal bulk scale reaction.

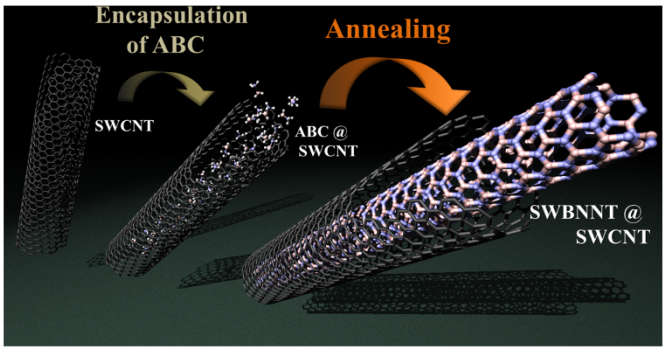

Figure 1 | Schematic images of the nano-templated reaction for the synthesis of thin SWBNNTs using internal nano-space of SWCNTs. Cap-opened single-wall carbon nanotube (SWCNT, left) is considered as a nano-scale container, and ammonia borane complexes (ABC) are introduced into them to form ABC encapsulated SWCNT (ABC@SWCNT, center). Then, the ABC@SWCNT is annealed at high-temperature under the vacuum to form single-wall boron nitride nanotube (SWBNNT) structure inside SWCNT (SWBNNT@SWCNT, right). B and N atoms are illustrated as pink and purple spheres, respectively.

Results

Encapsulation of ABC molecules in SWCNTs. We used arc-grown SWCNTs[5] having a diameter distribution of 1.4 ± 0.1 nm as a template to synthesize thin SWBNNTs. The uniform diameter distribution of SWCNT-templates is essential to realize a diameter selective synthesis of BNNTs; we can expect the thin SWBNNTs with typical diameter of 0.7 ± 0.1 nm using such SWCNTs. The encapsulation of ABC into SWCNTs was performed according to the previously reported gas phase process[18,19]. After the encapsulation of ABC molecules, ends of SWCNTs were capped by C_{60} molecules in order for ABC not to escape from SWCNTs in the ensuing process[46]. The sample was then washed with deionized water for 10 hours to remove surface-attached ABC molecules.

Figure 2a shows a low-magnification transmission electron microscope (TEM) image of ABC@SWCNTs. As clearly seen, the surface of SWCNTs is very clean showing an almost complete removal of residual ABC on the nanotube surface. High-magnification images in Figs. 2a and b show that short linear contrasts are observed along the SWCNTs axis. Electron energy loss spectra (EELS) obtained in the area presented as an inset of Figure 2d shows the presence of strong peaks at 197, 284 and 400 eV that are assigned to *K*-edge absorption of boron, carbon and nitrogen, respectively (Fig. 2d). The atomic ratio calculated from the background subtracted EELS spectrum (shown as red spectra in Fig. 2d) is B : C : N = 10 : 81 : 9. The ideal atomic ratio calculated assuming a closed packing structure of ABC molecules in (14, 7) SWCNTs (the structure is shown in supplementary Fig. S2) is B : C : N = 8 : 84 : 8 which well reproduces the observed atomic ratio. On the basis of these results, we conclude that the observed short linear contrasts in the SWCNTs should arise from encapsulated ABC molecules and that the filling yield of ABC molecules is very high.

Nano-templated reaction and structure characterization. ABC@SWCNTs was annealed at 1673 K for 3 days in vacuo; hereafter we refer to the annealed ABC@SWCNTs as a-ABC@SWCNTs. Figures 3a, b and c show TEM images of the a-ABC@SWCNTs. The low-magnification TEM image (Fig. 3a) shows that the surface of the sample is clean without any residual surface attached ABC molecules after the annealing process. Figures 3b and 3c are typical high-magnification TEM images of the a-ABC@SWCNTs, where the inner tube formation is clearly confirmed. Figure 3d is the corresponding EELS spectrum from isolated a-ABC@SWCNT (shown in the inset of Fig. 3d), indicating the presence of signals arising from B, C and N *K*-edges. The EELS spectra shows several peaks that are assigned to π*, σ* and fine structures. The observed conspicuous spectral shape of π* and σ* peaks in boron and carbon *K*-edge signals is characteristic to sp^2 bonding of hexagonal boron nitride and graphene sheets. The ratio of integrated intensities of π* (I_{π^*}) and σ* (I_{σ^*}) at the Boron *K*-edge (189–194 eV and 197–207 eV, respectively) represents the bonding environment of boron; the ratio of I_{π^*}/I_{σ^*} increases as sp^2 bonding character increases. The observed I_{π^*}/I_{σ^*} of a-ABC@SWCNT and ABC@SWCNT is 0.36 and 0.32, respectively, which is consistent with the idea that ABC molecules decompose and fuse to form BNNTs inside SWCNTs. Furthermore, the observed atomic ratio of B, C and N is found to

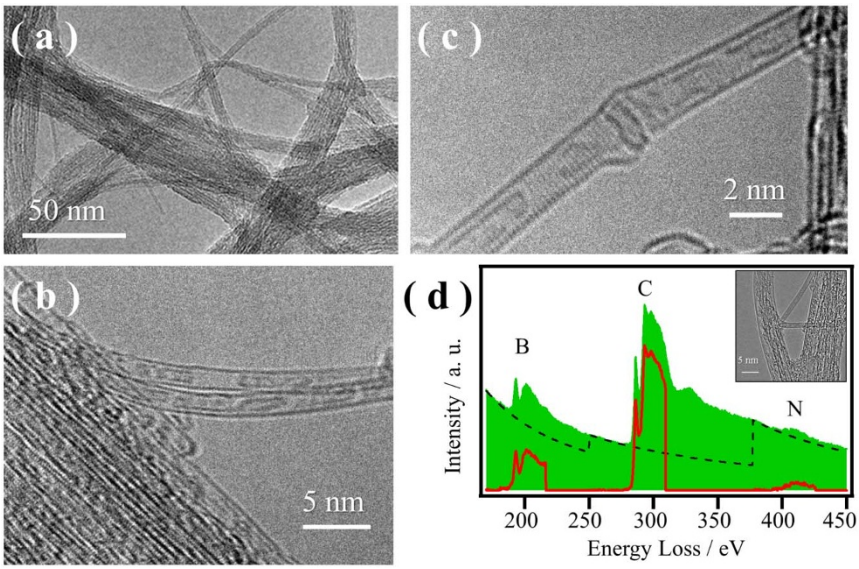

Figure 2 | TEM images and EELS spectrum of ABC@SWCNTs. (a) Low magnification TEM image of ABC@SWCNTs. No any impurities can be confirmed on the surface of the sample. (b), (c) High magnification TEM images of ABC@SWCNTs. Something amorphous like structures can be confirmed inside SWCNTs. (d) EELS spectrum of ABC@SWCNTs taken at inset region. Green filled spectrum, black dashed line, and red solid line correspond to the original spectrum, background comes from Zero-loss or plasmon peaks, and the background subtracted data from the original spectrum, respectively.

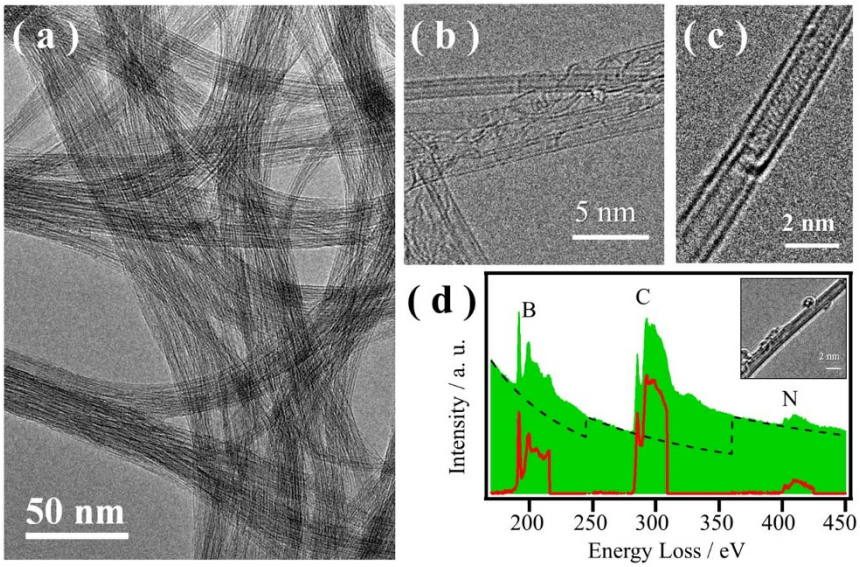

Figure 3 | TEM images and EELS spectrum of a-ABC@SWCNTs. (a) Low magnification TEM image of a-ABC@SWCNTs. No any impurities can be confirmed on the surface of the sample. (b), (c) High magnification TEM images of a-ABC@SWCNTs. double-wall like structures can be confirmed. (d) EELS spectrum of an a-ABC@SWCNT taken at inset region. Green filled spectrum, black dashed line, and red solid line correspond to the original spectrum, background comes from Zero-loss or plasmon peaks, and the background subtracted data from the original spectrum, respectively.

be 14 : 71 : 15 which is comparable to an expected atomic ratio of B : C : N = 17 : 66 : 17; to calculate the expected atomic ratio, we employ (6,5) SWBNNT@(14,7) SWCNT as a typical product having inner and outer diameters of 0.76 and 1.45 nm, respectively (the diameters were calculated using C-C distance of 1.42 Å[47] and B-N distance of 1.44 Å[48]). In addition to the characteristic π* and σ* peaks, a new peaks arising from π plasmon of BNNTs is observed at energy loss of 7.0 eV in an EELS spectrum of a-ABC@SWCNT (supplementary Fig. S3). These results strongly support a successful fabrication of SWBNNT inside SWCNTs (i.e., SWBNNT@SWCNTs).

To investigate the structure of a-ABC@SWCNT in detail, we performed high magnification TEM observation. Figure 4a is a high magnification TEM image of the sample, where lattice fringes arising from the atomic structure of the specimen are visible. The observed lattice image is similar to that of the moiré patterns usually observed in double wall CNTs[49,50], indicating that a tubular structure possessing honeycomb network is formed inside SWCNT; the diameters of the outer and inner tube are determined to be 1.45 and 0.80 nm, respectively. The observed lattice image and diameter are consistent with the formation of a double-wall nanotubes with chiralities of (6,5) and (12,10) for the inner BN and outer carbon nanotubes, respectively (supplementary Fig. S4). A multi-slice-based TEM image simulation of (6,5) BNNT@ (12,10) CNTs well reproduce the observed image (Figs. 4a and b), which strongly supports the formation of thin SWBNNTs in SWCNTs. To further obtain information on the detailed structure of BNNT@CNT, we conducted linear EELS mapping along the line perpendicular to the nanotube axis.

Figures 5a and b show, respectively, TEM and high angle annular dark field (HAADF)-Scanning TEM (STEM) images of annealed ABC@SWCNT taken at the same location, where an inner tube can be clearly observed. The diameters of the inner and outer tube are determined to be 0.77 and 1.45 nm, respectively, judging from the TEM image. An EELS mapping along the arrow shown in Fig. 5b is presented in Fig. 5c, consisting of 116 EELS spectra with a spatial step of 0.3 nm. In the EELS map, B, C and N *K*-edge spectra are clearly observed around 190, 290 and 400 eV, respectively. Figure 5d provides line profiles of the EELS map at the energy of 191.0, 284.6 and 405.4 eV corresponding to 1s → π* transitions of B, C and N *K*-edge EELS spectra, respectively. Figures 5d top, middle and bottom, respectively, show the line profiles of B, C and N after a subtraction of background due to the tails of zero loss and plasmon loss peaks. The observed line profiles of B and N are narrower than that of C, indicating that the inner tube is boron nitride and the outer tube is carbon. Two peaks observed at 1.14 and 2.58 nm in C-distribution correspond to side wall of outer SWCNTs[51], consistent with the diameter of outer tube determined from the TEM image. Widths of B- and N- line profiles are ca. 0.7 nm, which is also in good agreement with the diameter of the inner tube determined from the TEM image. Furthermore, the interlayer distance between the inner and outer tube determined from the liner profile is

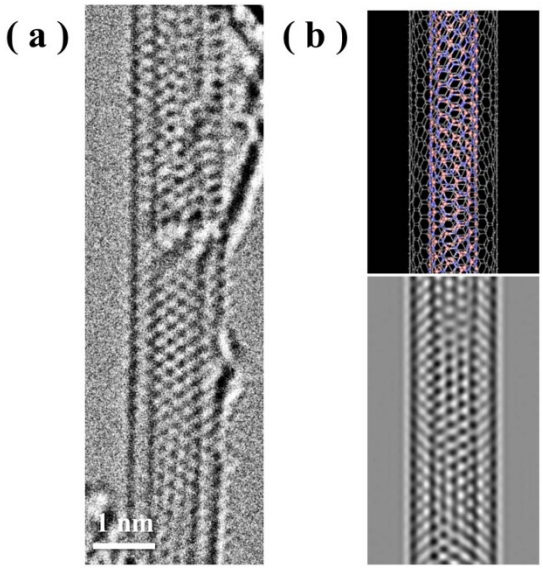

Figure 4 | High resolution TEM image of a double-wall nanotube observed in a-ABC@SWCNTs and the structure estimation. (a) High magnification CS corrected TEM image of obtained double wall like nanotube having diameter of 1.45 nm outer tube and 0.80 nm inner tube. (b) Structure model (above) and it's simulated TEM image (below) of (7,5) SWBNNT encapsulated in (12,10) SWCNT.

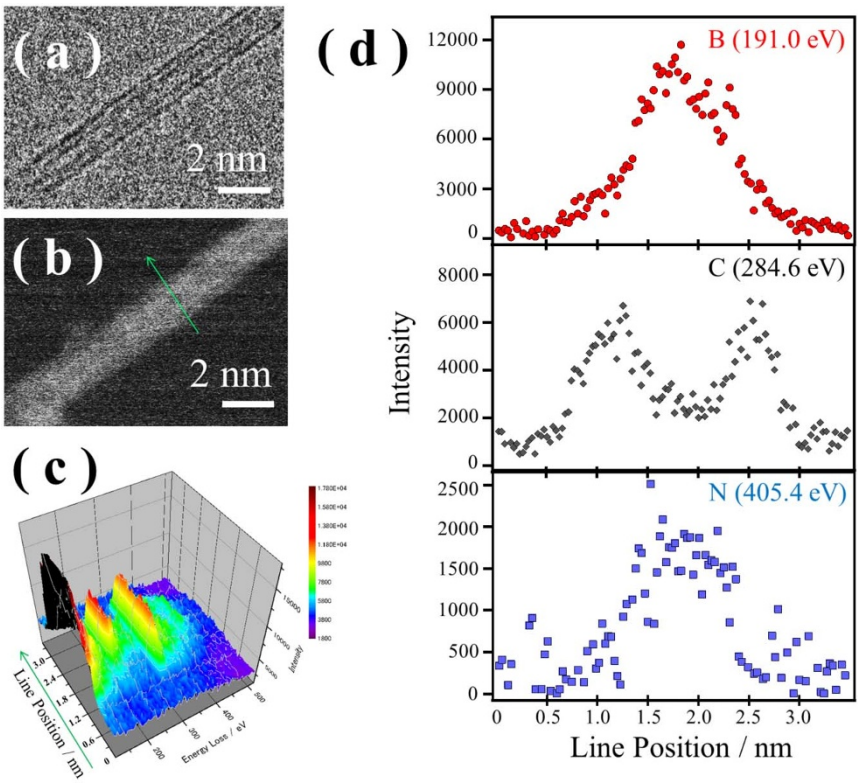

Figure 5 | HAADF-STEM images and STEM-EELS analysis of a SWBNNT@SWCNT. (a) Bright field TEM image of a double wall like nanotube having diameter of 1.45 nm outer tube and 0.77 nm inner tube, and (b) HAADF-STEM image at the same nanotube. (c) Linear EELS mapping spectrum along the green arrow in (b), in which the length is 3.48 nm and the energy-loss is from 110 to 519.4 eV. (d) Line profile of the EELS map cut at the energy of 191.0 eV (red circle), 284.6 eV (gray quarry) and 405.4 eV (blue square), which are correspond to the B *K*-edge, C *K*-edge, and N *K*-edge, respectively.

0.33 – 0.36 nm, which are similar to the typical interlayer distance of double-wall CNTs of 0.335 nm. All these results jointly show that thin BNNT nanotubes are formed in high yield inside the template made of SWCNTs.

Discussion

As shown above, the filling yield of ABC molecules in ABC@SWCNT is high; the atomic ratio of B, C and N is close to that of closed packing structure of ABC molecules in SWCNTs. However, the atomic ratio of B (or N) to C in an ideal SWBNNT@SWCNT should be 2.7 times higher than that of the closely packed ABC@SWCNT, suggesting that the number of boron and nitrogen atoms in ABC@SWCNT is insufficient to form a perfect SWBNNT having the same tube length as that of the SWCNT template. There should be, thus, single-wall area in a SWBNT@SWCNT double-wall nanotube, which has actually been observed in many TEM images.

Assuming that all ABC molecules react to form BNNTs inside SWCNTs, the theoretical ratio between double-wall and single-wall nanotube regions in the SWBNNT@SWCNTs is calculated to be 37 : 67. To obtain experimental information on the ratio and diameter distribution, we have performed a TEM-based statistical analysis using 102 isolated nanotubes; partially filled nanotubes were excluded from this analysis. Figure 6 shows a histogram showing the diameter distribution of SWCNTs (Fig. 6a, blue), inner SWBNNTs (Fig. 6b, green) and outer SWCNTs (Fig. 6b, red). The observed ratio of double-wall nanotubes to single-wall nanotubes is found to be 54 : 47, which is comparable to the theoretical ratio of double-wall and single-wall regions; the probability of finding double-wall and single-wall nanotubes is assumed to be proportional to the theoretical ratio between double-wall and single-wall regions. Considering the statistical error in the TEM-based sampling analysis, we conclude that the most of ABC molecules react to form BNNTs inside SWCNTs. The present nano-templated reaction proceeds very efficiently, which leads to the first production of thin SWBNNT in bulk scale; 0.5 mg of SWCNTs was typically used to obtain ca. 0.2 mg of the thin SWBNNTs (supplementary Fig. S5).

One of the most important aspects of the present reaction is that volatile ABC molecules remain inside SWCNTs to react each other under vacuum at high-temperature conditions. The main reason for this highly efficient formation reaction of BNNTs is that the end capping using C_{60} molecules prevents the encapsulated ABC molecules from escaping during the fusion reaction under vacuum high-temperature condition. The smallest diameter of SWBNNT formed in this reaction is 0.43 nm, which is close to the diameter of the thinnest stable SWBNNT; the ab-initio density functional theory (DFT) calculation on BNNTs and BN stripes shows that a (5,0) BNNT with a diameter of 0.4 nm is the thinnest stable BNNT[27]. BNNTs is found to possess the diameter of 0.7 $\pm$ 0.1 nm, and, to the best of our knowledge, this is the thinnest SWBNNTs synthesized in bulk scale so far.

The DFT study also predicts that the band gap of BNNTs does not vary depending on diameter and chirality (the predicted LDA band gap is about 4 eV) when a diameter of BNNT is larger than 0.6 nm[25]. It is well known that the LDA calculation normally underestimates the band gap, which is predicted to be 5.5 eV after the quasiparticle correction[26]. The previous experimental studies have shown that thick BNNTs have the band gap of 6 eV[33], which is in good agreement with the theoretical calculation. Thin BNNTs synthesized in this study have an average diameter of 0.7 nm, and therefore, the thin BNNTs are also expected to possess a band gap close to 6 eV. Figure 7 shows absorption spectra of SWBNNT@SWCNT and SWCNT, where the intensity of absorption is normalized at 280 nm; the

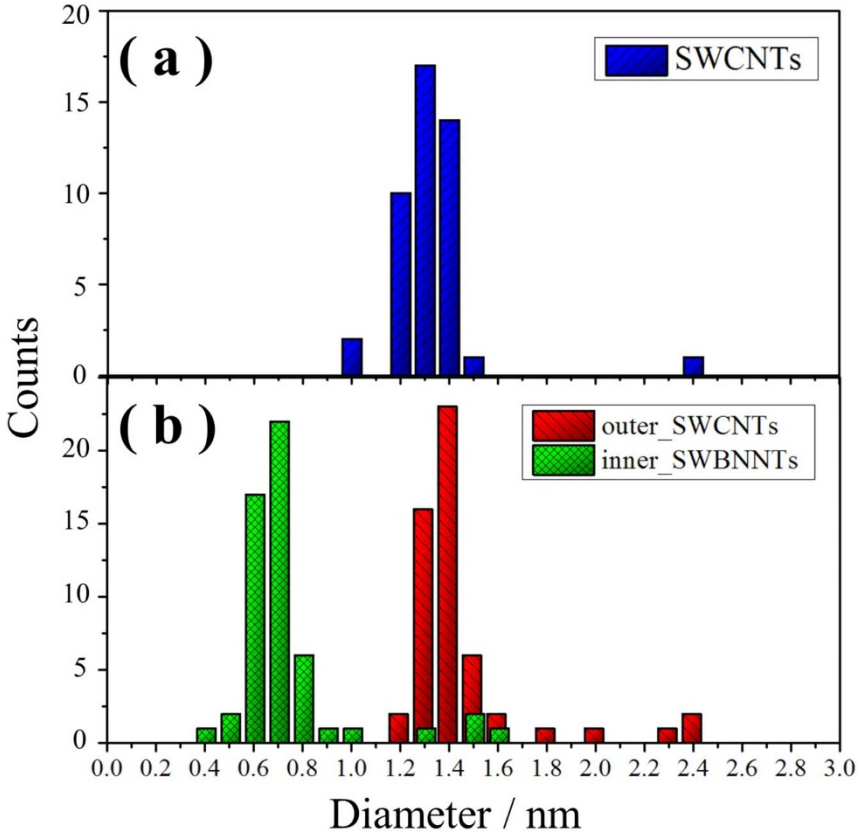

Figure 6 | Diameter distribution of obtained samples. (a) Diameter distribution of SWCNTs found in the samples, which is obtained by counting totally 47 single-wall nanotube regions. (b) Diameter distribution of SWBNNT@SWCNTs found in the samples, which is obtained by counting totally 54 double-wall nanotube regions. Red bars show diameter distribution of outer SWCNTs, and green bars show that of inner SWBNNTs.

sample was dispersed in 1,2-dichloroethane and the dispersion solution was sprayed onto the quartz substrate to obtain the absorption spectra. Apparently, in the absorption spectra of SWBNNT@SWCNT, a new peak appears at 6.1 eV that can be assigned to transitions due to π-π* bands of the BNNTs, indicating that thin BNNTs have a band gap of around 6 eV, which is in good agreement with the theoretical prediction[26,27]. Raman spectra (supplementary Fig. S6) shows that the interaction between SWCNTs and SWBNNTs is small, which is consistent with the large band gap of BNNTs.

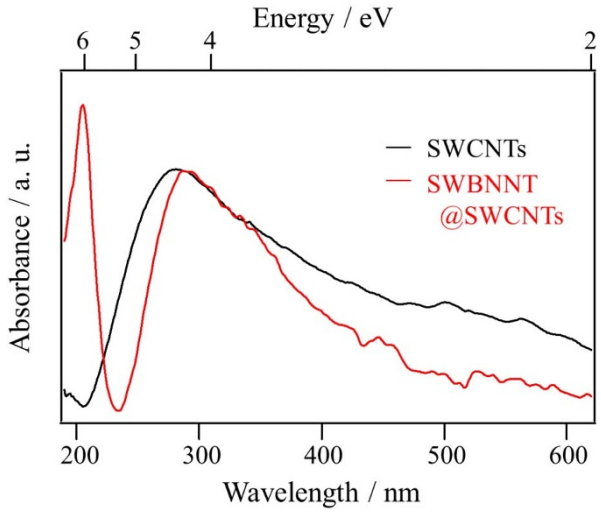

Figure 7 | Absorption spectroscopy of SWCNTs and SWBNNT@SWCNTs. These absorption spectra of SWCNTs (black) and SWBNNT@SWCNTs (red) were obtained by making thin films of them onto SiO_2 substrates, and measuring them between 620 – 190 nm wavelength, which correspond to 2.0–6.5 eV in the energy.

In summary, we have synthesized thin SWBNNTs with a narrow diameter distribution of 0.7 ± 0.1 nm using internal nanospace of SWCNTs as a nano-scale reactor. TEM, HAADF-STEM, EELS and EELS mapping using an aberration-corrected TEM have clearly shown the successful formation of SWBNNTs inside SWCNTs. In particular, the high resolution EELS mapping have proven to be a powerful technique to characterize the structure of the sample. Optical absorption measurements reveal that the band gap of the SWBNNTs is about 6 eV; The SWBNNTs is an ideal nanoscale template with a thin inter-cylinder space of 0.4 nm having stable structures, which is transparent to visible light. The nano-templated reaction used in this study can provide novel nanostructures that have been difficult to be synthesized by the conventional bulk-scale reactions. The current finding provides brand-new fields for further understanding on 1D nanosystems.

Methods

Preparation of samples. SWCNTs have been purchased from Meijo Nano Carbon Co. Ltd. and used after purification of heating at 1,473 K for 2 days under high vacuum (10^{-5} Torr). The purified SWCNTs were heated under dry airflow at 873 K for 30 min in order to remove the end-cap. ABC (97%, Sigma-Aldrich, Inc.) was annealed at 393 K for 12 hours to remove impurities. The annealed ABC was, then, sealed into a glass tube with cap-opened SWCNTs under high vacuum (10^{-6} Torr) followed by a heat treatment at 823 K for 3 days. After capped with those ends with C_{60} molecules and washed with deionized water for 10 hours, ABC encapsulated SWCNTs (ABC@SWCNTs) were annealed at 1673 K for 3 days. In addition to ABC molecules, 2,4,6-Trichloroborazine ($B_3Cl_3H_3N_3$; Sigma-Aldrich, Inc.) was also used as a precursor (supplementary Fig. S7).

Characterizations. For structural characterization of obtained samples, TEM observations were performed using a high-resolution field-emission gun TEM (JEOL

JEM-2100F, and Oxford's OJ JEOL 2200MCO with a CEOS probe and image aberration correctors). HAADF-STEM and EELS measurements were performed using JEOL JEM-ARM200F with a CEOS probe and image aberration correctors. All of these TEM observations were carried out using an acceleration voltage of 80 keV at room temperature. The sample was dispersed in DCE by the weak sonication for 1 hour with an ultrasonic bath sonicator. The solution was then dropped onto a copper grid coated with thin carbon film. The sample was heated at 300°C under vacuum for 30 min to remove DCE and water just before the TEM observations. TEM images were recorded with a charge coupled device with an exposure time of typically 1 s. All TEM image simulations have been performed using the WinHREM™ simulation software package released by HREM Research Inc. For absorption spectroscopy, the samples were dispersed in ethanol (99.5%, Wako) with ultrasonication for 1 hour, and then the dispersion solution was sprayed onto SiO_2 substrate to make thin films. The absorption spectra were measured with a UV-vis-NIR spectrophotometer (JASCO V-570) at room temperature. Raman spectra were measured with HR-800 spectrometer (Horiba Jobin Yvon) using excitation wavelengths at 488 and 633 nm.

1. Iijima, S. & Ichihashi, T. Single-shell carbon nanotubes of 1-nm diameter. *Nature* **363**, 603–605 (1993).
2. Saito, R., Fujita, M., Dresselhaus, G. & Dresselhaus, M. Electronic structure of chiral graphene tubules. *Appl. Phys. Lett.* **60**, 2204–2206 (1992).
3. Hamada, N., Sawada, S. & Oshiyama, A. New one-dimensional conductors: Graphitic microtubules. *Phys. Rev. Lett.* **68**, 1579–1581 (1992).
4. Thess, A. *et al.* Crystalline ropes of metallic carbon nanotubes. *Science* **273**, 483–487 (1996).
5. Ando, Y. *et al.* Mass production of single-wall carbon nanotubes by the arc plasma jet method. *Chem. Phys. Lett.* **323**, 580–585 (2000).
6. Smith, B. W., Monthioux, M. & Luzzi, D. E. Encapsulated C_{60} in carbon nanotubes. *Nature* **396**, 323–324 (1998).
7. Hirahara, K. *et al.* One-Dimensional Metallofullerene Crystal Generated Inside Single-Walled Carbon Nanotubes. *Phys. Rev. Lett.* **85**, 5384–5387 (2000).
8. Warner, J. H. *et al.* Rotating fullerene chains in carbon nanopeapods. *Nano Lett.* **8**, 2328–2335 (2008).
9. Nishide, D. *et al.* Single-wall carbon nanotubes encaging linear chain $C_{10}H_2$ polyyne molecules inside. *Chem. Phys. Lett.* **428**, 356–360 (2006).
10. Zhao, C., Kitaura, R., Hara, H., Irle, S. & Shinohara, H. Growth of Linear Carbon Chains inside Thin Double-Wall Carbon Nanotubes. *J. Phys. Chem. C* **115**, 13166–13170 (2011).
11. Okazaki, T. *et al.* Coaxially Stacked Coronene Columns inside Single-Walled Carbon Nanotubes. *Angew. Chem. Int. Ed.* **123**, 4955–4959 (2011).
12. Fujihara, M. *et al.* Dimerization-Initiated Preferential Formation of Coronene-Based Graphene Nanoribbons in Carbon Nanotubes. *J. Phys. Chem. C* **116**, 15141–15145 (2012).
13. Guan, L., Shi, Z., Li, M. & Gu, Z. Ferrocene-filled single-walled carbon nanotubes. *Carbon* **43**, 2780–2785 (2005).
14. Shiozawa, H. *et al.* A Catalytic Reaction Inside a Single-Walled Carbon Nanotube. *Adv. Mater.* **20**, 1443–1449 (2008).
15. Kitaura, R. *et al.* High yield synthesis and characterization of the structural and magnetic properties of crystalline $ErCl_3$ nanowires in single-walled carbon nanotube templates. *Nano Res.* **1**, 152–157 (2008).
16. Kobayashi, K., Suenaga, K., Saito, T., Shinohara, H. & Iijima, S. Photoreactivity preservation of AgBr nanowires in confined nanospaces. *Adv. Mater.* **22**, 3156–3160 (2010).
17. Muramatsu, H. *et al.* Synthesis and isolation of molybdenum atomic wires. *Nano Lett.* **8**, 237–240 (2008).
18. Kitaura, R., Imazu, N., Kobayashi, K. & Shinohara, H. Fabrication of metal nanowires in carbon nanotubes via versatile nano-template reaction. *Nano Lett.* **8**, 693–699 (2008).
19. Kitaura, R. *et al.* High-yield synthesis of ultrathin metal nanowires in carbon nanotubes. *Angew. Chem. Int. Ed.* **48**, 8298–8302 (2009).
20. Philp, E. *et al.* An encapsulated helical one-dimensional cobalt iodide nanostructure. *Nat. Mater.* **2**, 788–791 (2003).
21. Nakanishi, R. *et al.* Electronic structure of Eu atomic wires encapsulated inside single-wall carbon nanotubes. *Phys. Rev. B* **86**, 115445 (2012).
22. Golberg, D., Bando, Y., Tang, C. C. & Zhi, C. Y. Boron Nitride Nanotubes. *Adv. Mater.* **19**, 2413–2432 (2007).
23. Golberg, D. *et al.* Boron nitride nanotubes and nanosheets. *ACS Nano* **4**, 2979–2993 (2010).
24. Ayala, P., Arenal, R., Loiseau, A., Rubio, A. & Pichler, T. The physical and chemical properties of heteronanotubes. *Rev. Mod. Phys.* **82**, 1843–1885 (2010).
25. Rubio, A., Corkill, J. L. & Cohen, M. L. Theory of graphitic boron nitride nanotubes. *Phys. Rev. B* **49**, 5081 (1994).
26. Blase, X., Rubio, A., Louie, S. G. & Cohen, M. L. Quasiparticle band structure of bulk hexagonal boron nitride and related systems. *Phys. Rev. B* **51**, 6868 (1995).
27. Xiang, H., Yang, J., Hou, J. & Zhu, Q. First-principles study of small-radius single-walled BN nanotubes. *Phys. Rev. B* **68**, 035427 (2003).
28. Chen, Y., Zou, J., Campbell, S. J. & Le Caer, G. Boron nitride nanotubes: Pronounced resistance to oxidation. *Appl. Phys. Lett.* **84**, 2430–2432 (2004).
29. Zhao, X., Ando, Y., Liu, Y., Jinno, M. & Suzuki, T. Carbon nanowire made of a long linear carbon chain inserted inside a multiwalled carbon nanotube. *Phys. Rev. Lett.* **90**, 187401 (2003).
30. Lourie, O. R. *et al.* CVD growth of boron nitride nanotubes. *Chem. Mater.* **12**, 1808–1810 (2000).
31. Ma, R., Bando, Y., Sato, T. & Kurashima, K. Growth, morphology, and structure of boron nitride nanotubes. *Chem. Mater.* **13**, 2965–2971 (2001).
32. Kim, M. J. *et al.* Double-walled boron nitride nanotubes grown by floating catalyst chemical vapor deposition. *Nano Lett.* **8**, 3298–3302 (2008).
33. Lee, C. H., Xie, M., Kayastha, V., Wang, J. & Yap, Y. K. Patterned growth of boron nitride nanotubes by catalytic chemical vapor deposition. *Chem. Mater.* **22**, 1782–1787 (2010).
34. Pakdel, A., Zhi, C., Bando, Y., Nakayama, T. & Golberg, D. A comprehensive analysis of the CVD growth of boron nitride nanotubes. *Nanotechnol.* **23**, 215601 (2012).
35. Golberg, D. *et al.* Nanotubes in boron nitride laser heated at high pressure. *Appl. Phys. Lett.* **69**, 2045–2047 (1996).
36. Yu, D. *et al.* Synthesis of boron nitride nanotubes by means of excimer laser ablation at high temperature. *Appl. Phys. Lett.* **72**, 1966–1968 (1998).
37. Lee, R. *et al.* Catalyst-free synthesis of boron nitride single-wall nanotubes with a preferred zig-zag configuration. *Phys. Rev. B* **64**, 121405 (2001).
38. Arenal, R., Stephan, O., Cochon, J. L. & Loiseau, A. Root-growth mechanism for single-walled boron nitride nanotubes in laser vaporization technique. *J. Am. Chem. Soc.* **129**, 16183–16189 (2007).
39. Chopra, N. G. *et al.* Boron nitride nanotubes. *Science* **269**, 966–966 (1995).
40. Terrones, M. *et al.* Metal particle catalysed production of nanoscale BN structures. *Chem. Phys. Lett.* **259**, 568–573 (1996).
41. Loiseau, A., Willaime, F., Demoncy, N., Hug, G. & Pascard, H. Boron nitride nanotubes with reduced numbers of layers synthesized by arc discharge. *Phys. Rev. Lett.* **76**, 4737–4740 (1996).
42. Cumings, J. & Zettl, A. Mass-production of boron nitride double-wall nanotubes and nanococoons. *Chem. Phys. Lett.* **316**, 211–216 (2000).
43. Oku, T., Narita, I. & Tokoro, H. Synthesis and magnetic property of boron nitride nanocapsules encaging iron and cobalt nanoparticles. *J. Phys. Chem. Solids* **67**, 1152–1156 (2006).
44. Stephan, O. *et al.* Doping Graphitic and Carbon Nanotube Structures with Boron and Nitrogen. *Science* **266**, 1683–1685 (1994).
45. Kohler-Redlich, P. *et al.* Stable BC_2N nanostructures: low-temperature production of segregated C/BN layered materials. *Chem. Phys. Lett.* **310**, 459–465 (1999).
46. Shao, L., Lin, T. W., Tobias, G. & Green, M. L. H. A simple method for the containment and purification of filled open-ended single wall carbon nanotubes using C_{60} molecules. *Chem. Commun.* 2164–2166 (2008).
47. Wildoer, J. W. G., Venema, L. C., Rinzler, A. G., Smalley, R. E. & Dekker, C. Electronic structure of atomically resolved carbon nanotubes. *Nature* **391**,59–62 (1998).
48. Wirtz, L., Rubio, A., de La Concha, R. A. & Loiseau, A. Ab initio calculations of the lattice dynamics of boron nitride nanotubes. *Phys. Rev. B* **68**, 045425 (2003).
49. Zhu, H., Suenaga, K., Hashimoto, A., Urita, K. & Iijima, S. Structural identification of single and double-walled carbon nanotubes by high-resolution transmission electron microscopy. *Chem. Phys. Lett.* **412**, 116–120 (2005).
50. Fukui, N. *et al.* Moiré image patterns on double-walled carbon nanotubes observed by scanning tunneling microscopy. *Phys. Rev. B* **79**,125402 (2009).
51. Suenaga, K. *et al.* Synthesis of nanoparticles and nanotubes with well-separated layers of boron nitride and carbon. *Science* **278**, 653–655 (1997).

Acknowledgements

This work has been supported by the Grant-in-Aids for Specific Area Research (Grant No. 19084008) on Carbon Nanotube Nano-Electronics and for Scientific Research S (No. 22225001) of MEXT of Japan. R.N. thanks the Japan Society for the Promotion of Science for a Research Fellowship for Young Scientists. We thank Dr. Takashi Yamaguchi for fruitful discussions on the synthesis of BNNTs.

Author contributions

R.N. performed the synthesis and spectroscopic characterization of the samples. R.N., R.K. and J.H.W. performed TEM experiments. R.N., R.K. and H.S. designed the study and co-wrote the paper. All authors discussed the results.

Additional information

Supplementary information accompanies this paper at http://www.nature.com/scientificreports

Competing financial interests: The authors declare no competing financial interests.

How to cite this article: Nakanishi, R. *et al.* Thin single-wall BN-nanotubes formed inside carbon nanotubes. *Sci. Rep.* **3**, 1385; DOI:10.1038/srep01385 (2013).